Cell-Type-Specific Proteomics Analysis of a Small Number of Plant Cells by Integrating Laser Capture Microdissection with a Nanodroplet Sample Processing Platform

Vimal K. Balasubramanian,[1] Samuel O. Purvine,[1] Yiran Liang,[2] Ryan T. Kelly,[2] Ljiljana Pasa-Tolic,[1] William B. Chrisler,[1] Eduardo Blumwald,[3] C. Neal Stewart Jr.,[4] Ying Zhu,[1,5] and Amir H. Ahkami[1,5]

[1]Environmental Molecular Sciences Laboratory (EMSL), Pacific Northwest National Laboratory (PNNL), Richland, Washington
[2]Department of Chemistry and Biochemistry, Brigham Young University, Provo, Utah
[3]Department of Plant Sciences, University of California, Davis, California
[4]Department of Plant Sciences, Center for Agricultural Synthetic Biology, University of Tennessee, Knoxville, Tennessee
[5]Corresponding author: *ying.zhu@pnnl.gov*; *amir.ahkami@pnnl.gov*

Plant organs and tissues contain multiple cell types, which are well organized in 3-dimensional structure to efficiently perform physiological functions such as homeostasis and response to environmental perturbation and pathogen infection. It is critically important to perform molecular measurements at the cell-type-specific level to discover mechanisms and unique features of cell populations that govern differentiation and respond to external perturbations. Although mass spectrometry–based proteomics has been demonstrated as an enabling discovery tool for studying plant physiology, conventional approaches require millions of cells to generate robust biological conclusions. Such requirements mask the cell-to-cell heterogeneities and limit the comprehensive profiling of plant proteins at spatially resolved and cell-type-specific resolutions. This article describes a recently developed proteomics workflow for studying a small number of plant cells by integrating laser capture microdissection, microfluidic nanodroplet–based sample preparation, and ultrasensitive liquid chromatography–mass spectrometry. Using poplar as a model tree species, we provide detailed protocols, including plant leaf and root tissue harvest, sample preparation, cryosectioning, laser microdissection, protein digestion, mass spectrometry measurement, and data analysis. We show that the workflow enables the precise identification and quantification of thousands of proteins from hundreds of isolated plant root and leaf cells.

Basic Protocol 1: Plant tissue fixation and embedding
Support Protocol 1: Preparation of 2.5% CMC solution
Support Protocol 2: Slow freezing of CMC blocks to avoid crack development in the block
Basic Protocol 2: Preparation of cryosections
Alternate Protocol: Using a vacuum manifold to dehydrate the cryosection slides (primarily for root tissues)
Basic Protocol 3: Laser capture microdissection of specific types of plant cells
Basic Protocol 4: Nanodroplet-based sample preparation for ultrasensitive proteomic analysis
Support Protocol 3: Fabrication of nanowell chips
Basic Protocol 5: Liquid chromatography and mass spectrometry

CURRENT PROTOCOLS
A Wiley Brand
Current Protocols e153, Volume 1
Published in Wiley Online Library (wileyonlinelibrary.com).
doi: 10.1002/cpz1.153

Keywords: cell-type-specific proteomics • laser capture microdissection • mass spectrometry • nanoPOTS • poplar

How to cite this article:
Balasubramanian, V. K., Purvine, S. O., Liang, Y., Kelly, R. T., Pasa-Tolic, L., Chrisler, W. B., Blumwald, E., Stewart, C. N., Zhu, Y., & Ahkami, A. H. (2021). Cell-type-specific proteomics analysis of a small number of plant cells by integrating laser capture microdissection with a nanodroplet sample processing platform. *Current Protocols*, *1,* e153. doi: 10.1002/cpz1.153

INTRODUCTION

Current knowledge in plant biology primarily relies on omics approaches conducted at the level of the entire plant, organ, or tissue. However, to improve our understanding of plant cells as a system, there is a critical need to move toward studies focusing on individual plant cell types (Libault, Pingault, Zogli, & Schiefelbein, 2017). Recently, single-cell RNA sequencing and genomics technologies have led to the discovery and classification of previously unknown cell states in plants (Ryu, Huang, Kang, & Schiefelbein, 2019; Tang & Tang, 2019; Yuan, Lee, Hu, Scheben, & Edwards, 2018). Yet, studies on proteins, as the major structural and functional determinants of cells, are often limited to whole tissue analyses, primarily due to the lack of a reliable and accurate cell-type-specific proteomics platform. Cell-type-specific proteomic technologies will enable the investigation of many biological mysteries, such as signaling mechanisms based on protein binding and post-translational modifications (Slavov, 2020) during plant developmental processes and responses to environmental perturbations. When coupled with genomics and metabolomics, proteomics will unveil cellular heterogeneity, cell-cell communication, and signaling networks in plant biology (Libault et al., 2017; Rhee, Birnbaum, & Ehrhardt, 2019) that have remained elusive for a long time.

Unlike genomics and transcriptomics, there are no global protein amplification methods available for proteomics. To enable the study of small numbers of plant cells, all the sample preparation and LC-MS analysis steps need to be carefully designed to maximize sample recovery and measurement sensitivity. Here, we provide a detailed technical description of our recently developed nanoPOTS technology (nanodroplet processing in one-pot for trace samples; Liang et al., 2018; Zhu, Duo et al., 2018; Zhu, Piehowski et al., 2018) for highly sensitive proteome analysis of a small number of plant cells isolated by laser capture microdissection (LCM). We used poplar (*Populus spp*.), a major bioenergy woody crop, as our model plant system. We isolated mesophyll and vascular cells from leaf tissue, and cortex and vascular cells from root tissue using cryosectioning and LCM. Following that, protein extraction and digestion were performed in microfabricated nanowells. The peptide mixtures were separated with low-flow liquid chromatography, and data were collected with high-resolution mass spectrometry for cell-type-specific proteomic analysis.

This article includes five basic protocols (Fig. 1). Basic Protocols 1 and 2 describe plant tissue collection, fixation, tissue embedding, and thin-section preparation at subzero temperature using a cryotome. Basic Protocol 3 provides detailed information on the use of laser capture microdissection for isolating specific cell types from plant tissues. This is followed by nanoPOTS-based sample preparation, including protein extraction and trypsin digestion into peptides (with high sample recovery) for ultrasensitive proteomic analysis, outlined in Basic Protocol 4. Finally, in Basic Protocol 5, an optimized protocol

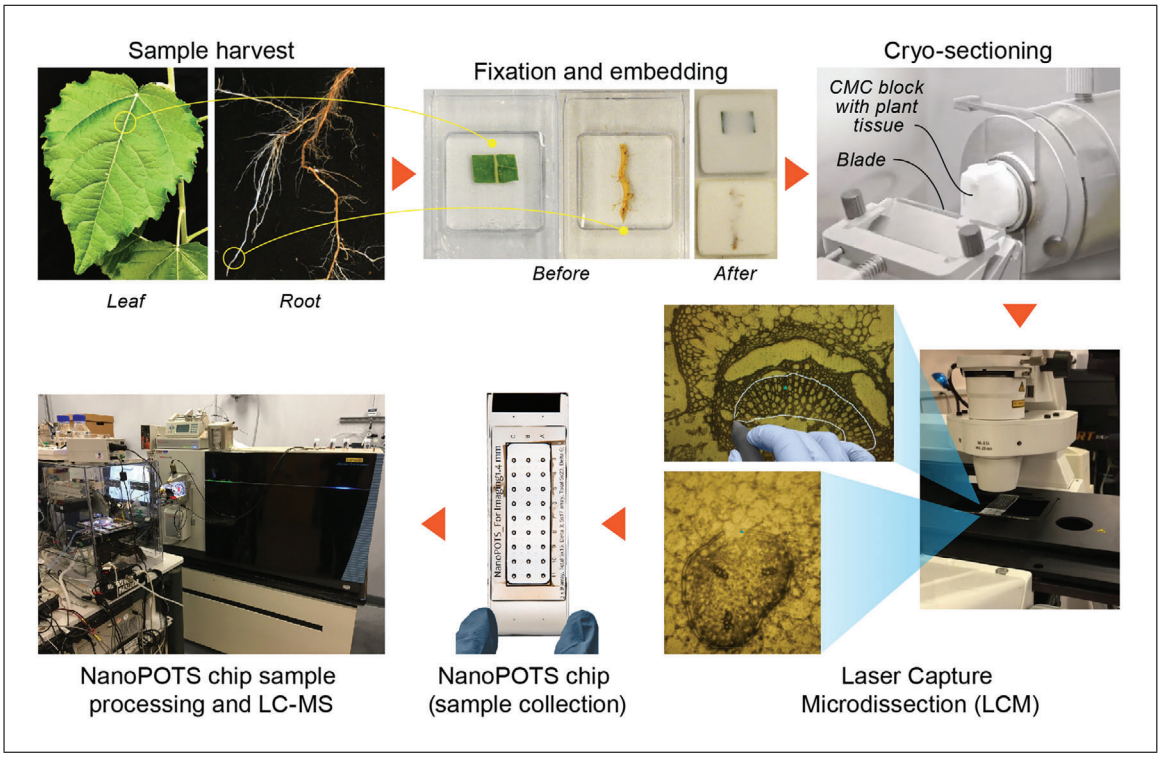

Figure 1 Pipeline for the cell-type-specific proteomics including sample harvest, fixation, embedding, cryosectioning, cell isolation with LCM, proteomic sample processing with nanoPOTS, measurement with LC-MS, and data analysis. nanoPOTS: nanodroplet processing in one-pot for trace samples.

for liquid chromatography and mass spectrometry is described for high-throughput and high-sensitivity analysis of plant cells.

PLANT TISSUE FIXATION AND EMBEDDING

BASIC PROTOCOL 1

Tissue fixation and embedding are the most critical steps for preserving the molecular state of cells and obtaining good histological tissue sections. The choice of fixative is very important, since the fixative generally arrests all biological processes in a cell and preserves the biomolecules such as DNA, RNA, and proteins. Precipitative fixatives like ethanol provide a good balance between histological resolution and recovery rate of the analytes (Milcheva, Janega, Celec, Russev, & Babál, 2013). In this work, we used a 3:1 ethanol:acetic acid fixative solution, which had been previously employed in proteomics sample preparation from plant tissues (Ahram et al., 2003; Collado-Romero, Alós, & Prieto, 2014). Ethanol dehydrates the tissue, thereby inhibiting all cellular reactions, whereas 25% acetic acid prevents tissue shrinkage due to the use of ethanol (Solomon & Varshavsky, 1985). To prevent cellular damage caused by the formation of ice crystals during the embedding process, the fixed tissue was cryoprotected using sucrose. The tissue fixation and embedding protocol presented here is carried out essentially as previously described (Matas et al., 2011; Zhu et al., 2016), with several modifications including extended fixation time, avoiding protease inhibitor during the sucrose infiltration step, and replacing OCT with CMC during the embedding process.

Materials

Fixation solution: 75% (v/v) ethyl alcohol (Millipore Sigma, cat. no. E7023) and 25% (v/v) acetic acid (Thermo Fisher Scientific, cat. no. A38S-500); maintained at 4°C

Populus tremula × *Populus alba*, clone INRA 717-1B4 (the original poplar cuttings were provided by Dr. Stephen DiFazio from West Virginia University. Clonal propagation of poplars was performed at EMSL)
10× phosphate-buffered saline (PBS), pH 7.4 (Invitrogen, cat. no. AM9624)
10% (w/v) sucrose (Thermo Fisher Scientific, cat. no. S25590) in 1× PBS (10 g sucrose in 100 ml PBS)
15% (w/v) sucrose in 1× PBS (15 g sucrose in 100 ml PBS)
2.5% carboxy methyl cellulose (CMC; see Support Protocol 1)
Dry ice
Liquid nitrogen

2-ml clean PCR microcentrifuge tubes (VWR, cat. no. 62111-754)
Razor blade or tissue puncher
Vacuum unit (Oxford Vacuum Pump, model no: GFS/VPZ0233) connected to vacuum desiccator (Thermo Fisher Scientific, cat. no. 5311-0250)
Spatula
Benchtop mixer: BD Clay Adams™ Nutator Mixer (BD Diagnostics, Model no: 421105)
Fisherbrand™ Disposable Base Molds (Thermo Fisher Scientific, cat. no. 22-363-554)
Forceps
Razor blades
0.5-ml microcentrifuge tubes

Leaf and root sample collection, fixation, and cryoprotection

1. Prepare fixation solution: 75% (v/v) ethanol and 25% (v/v) acetic acid. Place 1 ml fixation solution in a sufficient number of 2-ml microcentrifuge tubes and keep on ice.
2. Use a razor blade or a tissue puncher to harvest leaf or root tissue from *Populus tremula* × *Populus alba*, clone INRA 717-1B4 plants grown in pots filled with sandy soil in the greenhouse (or growth chambers).

   In our experiment, we harvested the midvein region of fully expanded leaves and 1 cm above root tips (see Fig. 1).
3. Wash the root tissue carefully with distilled water three times to remove adhering soil particles and contaminants.
4. Immediately transfer the harvested tissue into a microcentrifuge tube containing the fixation solution (step 1), maintaining the volume ratio of sample to fixation solution at ∼1:10. Place the tubes on ice and proceed with harvesting the remaining biological replicates.
5. Place the tubes containing the tissue and fixative solution in a vacuum unit and apply vacuum for 15 min.

   Vacuum treatment facilitates fixative infiltration and removal of air bubbles from the tissue.
6. Slowly release the vacuum to avoid tissue damage, and then place the tubes on ice. Use a pipette to remove the fixation solution from the tube and add 1 ml of fresh, ice-cold fixative solution again to the tubes. Place the tubes in a benchtop mixer [70 rotations per minute (rpm)] for 1 hr, kept at 4°C.
7. Remove the fixative solution and add 1 ml of fresh fixative to the tubes. Repeat steps 5 and 6.

8. Remove the fixative solution and wash the samples in ice-cold 1× PBS buffer by gently pipetting it into the tubes and mixing gently by inverting the tubes.
9. Gently transfer the tissue using a clean spatula to another microcentrifuge tube filled with 10% (w/v) ice-cold sucrose solution (which acts as a cryoprotectant) in 1× PBS. Place the tubes on ice immediately after exchanging the sucrose solution.
10. Place all the tubes on ice, transfer to the vacuum unit, and apply vacuum for 15 min.
11. Release vacuum slowly and gently transfer the tissue to a new tube filled with fresh, ice-cold 10% (w/v) sucrose solution in 1× PBS. Place the tube in a rotator kept at 4°C for 1 hr.
12. Remove the 10% sucrose solution and add 1 ml of freshly prepared, ice-cold 15% (w/v) sucrose in 1× PBS (15 g sucrose in 100 ml PBS buffer) to the tube. Repeat steps 10 and 11.
13. Once both 10% and 15% sucrose solution exchanges are completed, embed the tissues in the CMC matrix to prepare the tissues for cryosectioning, as described in the following steps.

Embedding the cryoprotected tissues using CMC

14. Transfer the sucrose-infiltrated tissue into a microcentrifuge tube filled with ice-cold 2.5% CMC solution. Gently shake the tube to remove the sucrose residue from the surface of the tissue.
15. For leaf tissues, place a plastic cryomold (labeled with sample information) on dry ice and fill it with 2.5% CMC solution. Quickly transfer the leaf tissue into the cryomold and freeze the mold using liquid nitrogen to make the frozen tissue CMC block.
16. Care should be taken while embedding the leaf tissue in 2.5% CMC solution, as the samples may not align correctly due to the less viscous nature of the 2.5% CMC solution. We recommend the use of forceps to hold the tissue in the correct orientation until the base of the block freezes and holds the sample in proper alignment.
17. While freezing the CMC block using liquid nitrogen, care should be taken not to overflow liquid nitrogen on top of the plastic mold, as liquid nitrogen can enter the CMC solution and cause air bubbles that can disturb the freezing process.
18. For root tissues, 0.5-ml microcentrifuge tubes are the preferred option compared to a plastic mold. Transfer the sucrose-infiltrated and CMC-washed root samples (as described in step 1) into 0.5-ml tubes containing 2.5% CMC solution and freeze in liquid nitrogen to make a solid block.
19. The frozen CMC blocks can be kept on dry ice while proceeding with the embedding of the remaining samples. Once all the blocks are made, they can be stored in a −80°C freezer until cryosectioning.
20. The frozen leaf blocks can be popped out from the plastic cryomold (after incubating the frozen blocks in cryotome for 20 min) by gently pressing the backside of the cyromold, while the frozen root block within the microcentrifuge tube can be popped out by cutting off the bottom of the microcentrifuge tube with a razor blade and pushing the root block out using a spatula.

PREPARATION OF 2.5% CMC SOLUTION

SUPPORT PROTOCOL 1

Carboxymethylcellulose (CMC) is a polymer of cellulose chains that can be dissolved in water up to a certain extent and used as an embedding matrix for cryosectioning. We observed that 2.5% CMC could be completely dissolved in water by mixing overnight under heated conditions. For plant tissues with low density (e.g., spike rachis, seeds), a higher

concentration of CMC (5%) can be used to avoid floating of tissues in the embedding matrix.

Materials

Carboxy methyl cellulose (CMC) (Sigma Aldrich, cat. no. 419273)
Ultrapure water prepared by Milli-Q Water Purification System.

MaxQ™ 4450 Benchtop Orbital Shaker (Thermo Fisher Scientific, Model no. SHKE4450)
500-ml plastic bottles

1. Heat 350 ml Milli-Q water in a 500-ml bottle and bring it up to 70°C. Add 10 g of CMC into the water. Place the bottle in an orbital shaker maintained at 90 rpm at 70°C and shake overnight to dissolve the CMC in water.
2. The next day, bring up the volume of the CMC solution to 400 ml by adding Milli-Q water and let it cool down at room temperature. This solution can be stored at 4°C for up to 4 weeks.

SUPPORT PROTOCOL 2

SLOW FREEZING OF CMC BLOCKS TO AVOID CRACK DEVELOPMENT IN THE BLOCK

The use of liquid nitrogen to freeze the sample during the embedding process could sometimes result in crack development in the embedding block that interrupts the sectioning process. So, we suggest an alternate way to freeze CMC blocks slowly, in case any difficulty arises with the regular approach (see Basic Protocol 1). In this alternate approach, a secondary liquid medium such as isopropanol is used. Isopropanol has a lower freezing point than water; hence, it will allow a gradual freezing process. This process needs to be conducted inside a fume hood, as isopropanol can evaporate at room temperature and cause irritation.

Materials

Isopropanol (Thermo Fisher Scientific, cat. no. A426P-4)
Dry ice
Tissue sample (see Basic Protocol 1)

250-ml beaker
Fisherbrand™ Disposable Base Molds (Thermo Fisher Scientific, cat. no. 22-363-554)
Forceps

1. Take 100 ml of isopropanol in a 250-ml glass beaker and place it inside the fume hood. Transfer some dry ice into the isopropanol beaker, which causes the dry ice to melt and creates a semi-frozen viscous isopropanol solution.

   This semi-frozen solution allows a slow and even freezing of the embedding block compared with liquid nitrogen.

2. Once the tissue sample is ready to be embedded, transfer the tissue into a cold plastic embedding mold (placed on dry ice) containing 2.5% CMC, and then use forceps to transfer the plastic mold into the semi-frozen isopropanol solution.
3. Care should be taken to prevent isopropanol from overflowing on top of the CMC solution.
4. The CMC block starts to freeze slowly. Once the block is nearly frozen, transfer it on to dry ice. Proceed with embedding the remaining samples and placing the blocks on dry ice.

Once all tissues are embedded into blocks, they can be stored in a −80°C freezer until cryosectioning.

PREPARATION OF CRYOSECTIONS

BASIC PROTOCOL 2

Cryosectioning is the process of making thin and frozen sections of tissues at subzero temperature. Cryosectioned tissues can be processed with LCM (laser capture microdissection) to isolate specific cell types (see Basic Protocol 3) for studying the changes associated with biomolecules such as RNA and proteins in the context of a given biology experiment (Hölscher & Schneider, 2008). The cryosectioning process is similar to conventional microtome-based sectioning, except that the entire sectioning unit is maintained at subzero temperature. The embedded tissue is mounted on a cryotome stage, which moves against a fixed blade in the micrometer range, resulting in thin sections of the tissue. The cryotome mounting stage and blade temperature can be adjusted for optimal sectioning (Marion, Bars, Satiat-Jeunemaitre, & Boulogne, 2017; Martin et al., 2016).

CAUTION: The cryotome instrument contains sharp blades; therefore, care should be taken while changing blades or positioning the blocks on the mounting stage. Cut-resistant gloves must be worn during the operation of the cryotome. Used blades must be disposed of in a sharps container.

Materials

RNaseZAP RNase decontamination solution (Invitrogen)
Ethyl alcohol (ethanol), pure. (Sigma Aldrich, cat. no. E7023)
Plastic mold containing frozen CMC tissue block (Basic Protocol 1 or Support Protocol 2)
Ultrapure water prepared by Milli-Q Water Purification System (Millipore Sigma)

Cryotome: CryoStar™ NX70 Cryostat (Thermo Fisher Scientific, SN: S18071458)
Thermo Scientific™ Specimen Stages 550 Series (Thermo Fisher Scientific, cat. no. 71-572-0).
MX35 Premier Disposable Low–Profile Microtome Blades (Thermo Fisher Scientific, cat. no. 89238-778)
PEN (polyethylene naphthalate) membrane glass slide (Carl Zeiss, PEN 1.0 Membrane Slides, cat. no. 415190-9041-000)
Spectrolinker XL-1000 UV Crosslinker UV source (Thomas Scientific, cat. no 1195T73)
Forceps and tweezers
Glass rod
Small paint brush
Dissecting microscope
Slide dipping jars
Stopwatch

Cryosectioning procedure to make thin tissue sections

1. Turn on the cryotome and maintain it in standby mode to reach optimal temperature (−20 °C) in the cryo-chamber. The specimen stage mounting station and blades are set to −14°C and −12°C, respectively. Clean the brush, spatula, and sectioning blade with RNaseZAP and 100% ethanol, and treat with UV light for 2 min.

2. Treat the PEN membrane−coated glass slides with UV for 30 min (as per manufacturer instruction), which helps the cryosections to better stick to the membrane. After the UV treatment, move all the PEN slides inside the cryochamber and let them cool down to the chamber temperature.

3. Put a specimen stage inside the cryotome and allow it to cool down. Meanwhile, move the plastic mold containing the frozen CMC tissue block from the −80°C freezer onto dry ice, and then transfer it into the cryotome. Allow the plastic mold to warm up for about 10 min (inside the cryotome), pop the embedded CMC tissue block out of the plastic mold, and leave it on the cryotome.

4. Transfer the CMC block onto the specimen stage in an upright position to enable a cross section of the embedded tissue. Add 1-2 ml of 2.5% CMC as supporting reagent at the bottom of the CMC block to freeze the block firmly onto the specimen stage. This prevents the CMC block from falling off during cryosectioning.

5. Install the specimen stage containing the CMC block onto the mounting station maintained at −14°C and leave it for 30 min to let the CMC block acclimate to the mounting station temperature.

   Note that the cryotome working temperature (see step 1) and incubating the block for 30 min is very critical to obtain unrolled and good cryosections.

6. Start cryosectioning to trim away the excess CMC material until the plant tissue is clearly visible. Using a section thickness of up to 50 µm, perform this trimming step slowly and watch for minor cracks presented in the block, which could develop into a major crack and break the block if the trimming process is performed too rapidly.

   We recommend performing this trimming process using the cryotome, as the CMC block can break unevenly when the trimming process is performed using a razor blade.

7. Adjust the section thickness to 12 µm, set the vacuum pressure to 50%, and start the sectioning process slowly and in parallel. Press a glass rod against the section to obtain un-rolled thin cryosections. Use a brush to transfer some test sections onto a glass slide and check under a microscope to make sure that the tissue sections are not rolled, and that cells are well organized on the tissue sections.

8. Repeat the sectioning process, gently transfer the sections onto a pre-cooled PEN membrane slide, and thaw the section quickly by placing a finger underneath the slide. Once completely thawed, the tissue will stick to the PEN membrane; immediately place the glass slide on the metal surface of the cryotome to freeze the tissue. If the sections curl, use a brush to gently unroll and thaw it completely onto the glass slide, and immediately freeze the glass slide.

9. Transfer multiple sections onto the PEN membrane slide, and keep the slide frozen during the process. Once the slides are filled with sections, proceed with ethanol washing (to remove CMC coating from the tissue), as described in the following steps

Slide wash step to dehydrate the tissue sections and to remove embedding material

Slide wash procedures are used to dehydrate the tissue sections. This procedure also removes the CMC coating on the tissue, which otherwise interferes in the LCM cell isolation process because it takes more laser energy and time to cut through the CMC layer. To remove the CMC coating from leaf tissue without affecting the protein yield, we use a series of ethanol wash steps. For the root tissue sections, the ethanol washes reduce overall protein yields, and thus we suggest using an alternate slide drying procedure (see Alternate Protocol). Prepare 70%, 85%, and 100% ethanol in separate slide dipping jars. Keep these wash solvents at −20°C until use.

10. Transfer the slide into the 70% ethanol (2 min), followed by 85% ethanol (1 min) and 100% ethanol (1 min). Between steps, the solvent residues are minimized by blotting the slide on absorbent paper. Use a stopwatch to monitor the time and use forceps to transfer the slides into each of the jars.

This process not only dehydrates the cells, but also helps to remove the CMC layer surrounding the sections, which was found to facilitate the LCM procedures.

11. Once the slide wash is complete, air-dry the slides on the bench for 5 min.

    The slides are now ready for LCM.

    Optional: The slides can be stored in −80°C freezer for up to 8 weeks. After taking the slides out of the freezer, if necessary, dehydrate with a vacuum manifold as mentioned in the Alternate Protocol.

USING A VACUUM MANIFOLD TO DEHYDRATE THE CRYOSECTION SLIDES (PRIMARILY FOR ROOT TISSUES)

ALTERNATE PROTOCOL

Vacuum drying is generally used to dry sensitive materials by reducing the chamber pressure below the vapor pressure of water, thereby enabling the water present in the material to evaporate quickly. In the case of leaf tissue sections, the above-described slide wash procedure was found to yield reasonable amounts of protein for proteomics analysis. However, in the case of root cells, the total protein yield was relatively low after slide washing. Therefore, for root tissues, we adopted a vacuum drying procedure and found that significantly higher amounts of protein were retained compared to the ethanol wash method.

Materials

Slides from cryotome (Basic Protocol 2)
Vacuum unit (Oxford vacuum pump, model no: GFS/VPZ0233) connected to vacuum desiccator (Thermo Fisher Scientific, cat. no. 5311-0250)

1. After the cryosectioning procedure, transfer the slides from the cryotome to inside the vacuum chamber to bring them to room temperature.
2. Turn on the vacuum unit and leave the slides for 15-20 min until the slides lose all moisture from the embedding material and become dry.
3. Remove the slides and proceed with the LCM process.

LASER CAPTURE MICRODISSECTION OF SPECIFIC TYPES OF PLANT CELLS

BASIC PROTOCOL 3

Laser capture microdissection (LCM) is a cell isolation technique to selectively harvest cells of interest from plant tissues using a high-energy laser beam. Cells of interest can be isolated based on their morphology, spatial location, and fluorescent labeling done using specific antibodies or transgenic techniques. LCM has been used to isolate underrepresented cell types such as trichomes, epidermal cells, root hairs, and root pericycle (Nestler, Schütz, & Hochholdinger, 2011; Schilmiller et al., 2010; Zhu et al., 2016), and to resolve the molecular complexities in heterogeneous cell populations of plant tissues. The whole LCM process is semi-automated, where a monochromatic laser light at higher energy is targeted on the fixed and cryosectioned tissue placed on a charged PEN membrane. The LCM technique, combined with high-resolution mass spectrometry, is a powerful tool to study the proteomic compositions of unique and specific cell types. In this protocol, we describe the isolation of a small number of cells directly into nanoliter-scale microfabricated wells, which will be used for highly efficient and sensitive proteomics analysis. The integration of nanoPOTS (nanodroplet processing in one pot for trace samples) technology with LCM was developed previously in our lab (Zhu, Dou et al., 2018).

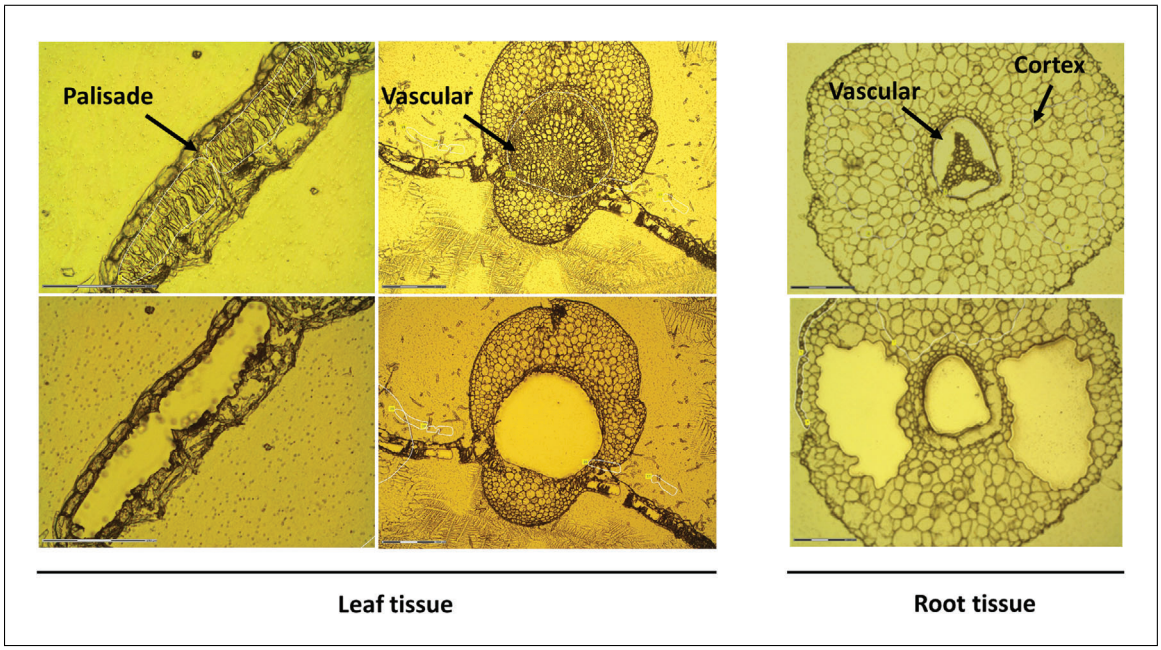

Figure 2 Laser capture microdissection–based cell isolation from the poplar leaf (palisade and vascular) and root (cortex and vascular) tissues. The top row shows tissue sections before LCM, and the bottom row shows tissue sections after LCM.

Materials

Ethanol-treated leaf slide (Basic Protocol 2) or vacuum-dried root slide (Alternate Protocol)
Dimethyl sulfoxide (DMSO), HPLC-grade (Fisher Scientific, cat. no. AA22914K7)

Laser-capture microdissection microscope (Zeiss PALM Microbeam)
Glass nanoPOTS chips with 1.4-mm-diameter nanowells (see Support Protocol 3)
The hydrophilic/hydrophobic patterned glass slide can also be purchased from Scientific Device Laboratory (Des Plaines, IL, U.S.A.)
SlideCollector 48 (Carl Zeiss)
Glass slides
Aluminum foil (Reynolds wrap, purchased from the local supermarket)

Laser-capture microdissection procedure to isolate leaf and root cells

1. Turn on the LCM microscope and open the PALMrobo software. Keep the system on for 15 min to stabilize the laser energy. Adjust the microscope and laser settings in the software as follows: Zoom: 20×; cut energy: 39; focus: 30; cycle number: 6; *z*-axis: 2 µm; and cut speed: 15. Set the catapulting energy to be 30 with a focus delta of 5.

   These settings were optimized for poplar leaf and root tissues and can be slightly adjusted to apply to other tissues of interest.

2. Transfer the ethanol-treated leaf slide or vacuum-dried root slide onto the slide adapter of the LCM microscope. Use the LCM marker pen to mark the region of interest containing a specific cell type in the section.

   We isolated palisade and vascular cell types from leaf tissue and cortex and vascular cell types from root tissue (Fig. 2). Using the LCM marker pen, we marked 35 palisade regions with an average area of 5000-7000 μm^2 per region, corresponding to 500-1000 cells per technical replicate. For vascular cells, 3-4 vascular regions with an average area of $2-4 \times 10^5$ μm^2 were marked, corresponding to 1000-2000 cells per technical replicate. For root cells, 14 cortex regions with an average area of 2.5×10^4 μm^2 per region, comprising

500-1000 cells per technical replicate, were marked. For root vascular cells, we marked 7 regions with an average area of 2×10^4 μm^2 per region, comprising 1000-2000 cells per technical replicate.

3. After marking all sections, select the "close-cut" option to start cutting those marked regions using the abovementioned laser conditions. It takes about 2 hr to finish cutting all the marked leaf cell types and 1 hr for the root cell types. The cut sections constitute 2 technical replicates from each biological replicate. In total, we collected leaf and root cells from 2-4 biological replicates, from each of which 2 technical replicates were collected.

4. Once these marked regions are cut, they are ready to be catapulted into the nanowells containing DMSO. The nanowells are loaded In advance with 300 nl of DMSO by using liquid handling robot. Bring the nanowell chip to room temperature and allow it to thaw for 5 min before sample collection. Mount the nanowell chip onto the 48-well slide holder (Slide Collector 48) of the LCM microscope. Adjust the focus of the microscope to make sure the DMSO droplet is aligned to the center at each dedicated location.

   CAUTION: *Care should be taken while handling DMSO to avoid spilling onto skin.*

5. Start the catapulting process for cell collection: high-energy laser spots are applied to the cut regions, which eject the tissue voxels into the DMSO droplets preloaded in nanowells.

   Since the nanoliter DMSO droplets will slowly evaporate at room temperature, the catapulting process should be performed as quickly as possible.

6. After all the tissue voxels are collected, cover the chip with a glass slide, wrap with aluminum foil, and place the nanowell chip in a -20°C freezer. For collecting additional samples on the same chip, bring the chip to room temperature only when new tissue regions are already cut and ready to be catapulted.

NANODROPLET-BASED SAMPLE PREPARATION FOR ULTRASENSITIVE PROTEOMIC ANALYSIS

BASIC PROTOCOL 4

To enable highly efficient and sensitive analysis of a limited amount of samples, such as a small number of plant cells isolated from LCM, we developed nanoPOTS (nanodroplet processing in one pot for trace samples; Liang et al., 2018; Zhu, Duo et al., 2018). The nanoPOTS platform simultaneously addresses two major challenges in conventional proteomics workflow: poor sample recovery and low protein digestion kinetics. The nanoPOTS platform consists mainly of two components, a microfabricated nanowell-array chip and a nanoliter-scale liquid handling robotic station. Most of our nanoPOTS chips were fabricated on glass substrates with hydrophilic/hydrophobic coating using a previously described protocol (Zhu, Dou et al., 2018). It should be noted that nanowell chips fabricated on other substrates—e.g., polypropylene (Dou et al., 2019; Lee et al., 2018)—should be readily adapted to the nanoPOTS platform. The operation of nanoPOTS employs a single-pot workflow, where all the proteomic processing steps are performed in a single nanowell without transferring to other containers. The single-pot protocol can efficiently minimize nonspecific adsorption−associated sample loss.

Materials

Nanowell chip containing LCM-isolated plant samples
Ultrapure water prepared by Milli-Q Water Purification System
n-Dodecyl β-D-maltoside (DDM; Sigma-Aldrich, cat. no. D4641-1G)
A stock DDM solution is prepared at 1% (m/v) in water and aliquotted at 20 µl per tube. The tube is stored in a -20°C freezer.

Dithiothreitol (DTT; No-Weigh™ Format; Thermo Scientific, cat. no. A39255)
10× phosphate buffered saline (PBS; Sigma Aldrich, cat. no. P5493-1 liter)
Ammonium bicarbonate (ABC) buffer, 50 mM, pH 8.5 (Sigma, cat. no. S2454)
Iodoacetamide, IAA (single-use, Thermo Scientific, cat. no. A39271)
Lys-C, Mass Spectrometry Grade (Promega, cat. no. V1671)
A stock Lys-C solution is prepared by dissolving 15 µg Lys-C in its resuspension buffer (provided with the Lys-C) at a concentration of 0.1 ng/nl, aliquotting 10 µl/tube, and storing in a −80°C freezer.
Trypsin, Mass Spectrometry Grade (Promega, cat. no. V5280)
A stock trypsin solution is prepared by dissolving 100 µg trypsin in 25 mM acetic acid at a concentration of 0.2 ng/nl, aliquotting 10 µl/tube, and storing in a −80°C freezer.
Formic acid, LC-MS grade (Thermo Scientific, cat. no. 28905)

A home-built nanoPOTS robotic liquid handling station; Alternatively, a commercially available nanoliter liquid dispensing station CellenONE (Cellenion SASU, France) can be used
Glass nanoPOTS chips with 1.4-mm-diameter nanowells (see Support Protocol 3)
The hydrophilic/hydrophobic patterned glass slide can also be purchased from Scientific Device Laboratory (Des Plaines, IL, U.S.A.).
75°C incubator
Glass slides
Aluminum foil (Reynolds wrap, purchased from the local supermarket)
Kimwipes
Sealable plastic box
Vacuum desiccator

System preparation

1. Turn on the nanoPOTS robotic station and initialize all the stages and syringe pump.
2. Check if there are visible bubbles inside the syringe. If so, remove the syringe from the pump, flush out the bubble by tapping the barrel, and fill it with purified water. Start the pump to flush out the bubble in the fluid path and capillary probe.
3. Turn on the humidifier and set the controller at 95% humidity. Allow the humidity in the robotic chamber to stabilize.

   The process usually takes 30 min to 1 hr, depending on the ambient temperature and humidity.

4. Bring out the nanowell chip containing LCM-isolated plant samples from the −20°C freezer and allow it to warm to room temperature before opening the aluminum foil.
5. Open the cover and place the nanowell chip in a 75°C incubator for 20 min to completely evaporate all the DMSO droplets in the nanowells.
6. Cover nanowell with glass slide and keep it on the benchtop to allow it to cool down to room temperature.

Proteomic sample preparation

7. Prepare cell lysis/protein extraction buffer by diluting DDM and DTT in a buffer containing 0.5× PBS and 25 mM ABC.

   The final concentrations of DDM and DTT are 0.2% (w/v) and 5 mM, respectively. The 0.5× PBS and 25 mM ABC buffer can be prepared by 1:1 mixing of 1× PBS buffer with 50 mM ABC buffer.

8. Mount the nanoPOTS chip on the robotic liquid handling system and align the well positions using three alignment points designed on the chip.

9. Dispense 150 nl cell lysis/protein extraction buffer in each nanowell using the robotic system.
10. Cover nanowell chip using glass slide and wrap chip with aluminum foil.
11. Prepare a humidified box by placing multiple layers of Kimwipes in a sealed plastic box and wetting the paper using purified water.
12. Place the nanoPOTS chip in the humidified box and incubate the box in a 75°C incubator for 60 min to lyse the cells and extract and reduce the proteins.
13. Bring out the humidified box and cool it down to room temperature before opening it.
14. Prepare protein alkylation solution containing 40 mM IAA in 50 mM ABC buffer.
15. Dispense 50 nl alkylation solution into each nanowell.
16. Wrap the chip with aluminum foil and incubate the alkylation reaction at room temperature for 30 min.
17. Prepare Lys-C digestion solution containing 0.01 ng/nl Lys-C in 50 mM ABC buffer.
18. Dispense 50 nl Lys-C digestion solution (0.5 ng) into each nanowell.
19. Wrap the chip with aluminum foil, place the chip in the humidified box, and incubate chip in 37°C incubator for 3 hr.
20. Bring out the humidified box and cool it down to room temperature before opening it.
21. Prepare trypsin digestion solution containing 0.02 ng/nl trypsin in 50 mM ABC buffer.
22. Dispense 50 nl trypsin digestion solution (1 ng) into each nanowell.
23. Wrap the chip with aluminum foil, place the chip in the humidified box, and incubate chip in 37°C incubator for 10 hr (overnight).
24. Bring out the humidified box and cool it down to room temperature before opening it.
25. Prepare 5% (v/v) formic acid solution in water.
26. Dispense 50 nl of 5% formic acid solution into each nanowell to quench the protease activity and acidify the sample.
27. Wrap the chip with aluminum foil and incubate the chip at room temperature for 30 min.
28. Open the chip and place in a vacuum desiccator for 30 min under vacuum to completely dry the samples in nanowells.
29. Wrap the chip with aluminum foil and store the chip in −20°C freezer before analysis.

FABRICATION OF NANOWELL CHIPS

SUPPORT PROTOCOL 3

The fabrication of glass chips involves multiple steps, including computer-assisted photomask design, photomask printing, transferring pattern to slide substrates using UV exposure, pattern development and chromium etching, glass etching with hydrofluoric acid, hydrophobic treatment with silane solution, and assembling glass spacer and cover slide. The protocol was initially reported in previous publications (Liu, Zhu, Feng, Fang, &

Fang, 2017; Zhu, Duo et al., 2018). We provide herein a general protocol to fabricate nanowell glass chip in a cleanroom using the instruments available in our laboratory. Note that the protocol may require slight modifications if alternative instruments are used. The hydrophilic/hydrophobic patterned glass slide can also be purchased from Scientific Device Laboratory (Des Plaines, IL, U.S.A.).

Materials

AZ400K developer (AZ Electronic Material USA Corp., Somerville, NJ)
N_2 source
Chrome etchant (CEP200, HTA enterprise, San Jose, VA)
Glass etching solution: mix 200 ml buffered NH_4-HF etchant solution (Sigma-Aldrich, cat. no. 40207), 400 ml HCl (Sigma-Aldrich, cat. no. 320331), and 400 ml water in a plastic container
CAUTION: *The HF-based etching solution is highly corrosive and toxic. Safety goggles, HF-protective gloves (neoprene or nitrile; 22 mil), and other personal protection equipment (PPE) should be used.*
AZ400K stripper (AZ Electronic Material USA Corp., Somerville, NJ)
Heptadecafluoro-1,1,2,2-tetrahydrodecyl-dimethylchlorosilane (PFDS, Gelest, cat. no. SIH5840.4)
2,2,4-trimethylpentane (Sigma-Aldrich, cat. no. 360066-2 liters)
Ethanol
Two-component epoxy (Devcon HP 250, Amazon)
Liquinox solution (Alconox, cat. no. 1232-1)

Computer running Autocad 2017
Photomasks containing nanowell patterns (made in house or through a vendor (e.g., Photo Sciences, Inc, Torrance CA)
1 × 3 inch-size glass substrate with chromium and AZ photoresist coating (Telic Company, Valencia, CA)
Photomask aligner (Neutronix-Quintel)
Hot plate
Kapton tape (Amazon, 1.5 in. wide)
Oxygen plasma system (AP-300, Nordson MARCH)
Thin glass coverslip (0.17 mm; Thermo Fisher Scientific , cat. no. 22X701)
Glass spacer (micromachined glass frame with 57 mm in length, 24 mm in width, and 1 mm in thickness; the internal space is 51 × 18 mm; GIN KOO MEMS Scientific & Technological Co. Ltd., Beijing, China)

1. The nanowell chip is designed using Autocad 2017. To match the PALM Microbeam LCM microscope, a total of 27 nanowells (3 rows and 9 columns) are included in one chip. The well-to-well distance is set at 4.5 mm in both the *x* and *y* directions.

   Photomasks can be generated in house using a direct-write lithography system (SF-100, Intelligent Micro Patterning LLC) or through a vendor (Photo Sciences, Inc, Torrance CA).

2. Align the glass substrate coated with chromium and AZ photoresist with the photomask using a photomask aligner, and flood with UV light for 10 s using the UV lamp that is part of the photomask aligner.

   The optimal exposure time may vary depending on the UV lamp intensity levels.

3. Develop the AZ photoresist by putting the glass substrate in AZ400 developer for ∼1 min. Gently shake the container until the patterns are visible. Rinse the substrate with purified water and dry it with nitrogen.

4. Etch the exposed chromium layer by putting the glass substrate in chrome etchant for 1–2 min. Inspect the substrate to make sure that the chromium layer is completely etched. Rinse the substrate with purified water and dry it with nitrogen.
5. Bake the substrate at 110°C for 15 min on a hot plate to denature the photoresist and solidify the pattern.
6. Cool down the substrate to room temperature and use Kapton tape to cover the back side and the edges of the glass substrate.
7. Etch the substrate using the glass etching solution for 10 min on an orbital shaker to generate microstructure with a depth/height of ~10 μm. Rinse the substrate and dry it with nitrogen.

   CAUTION: *The HF-based etching solution is highly corrosive and toxic. Safety goggles, HF-protective gloves (neoprene or nitrile; 22 mil), and other personal protection equipment (PPE) should be used. The etching should be performed in a dedicated fume hood.*
8. Remove the Kapton tape and remove the remaining AZ photoresist by putting it in AZ400 stripper for 5 min with gentle shaking.
9. Rinse the glass substrate with purified water, dry it with nitrogen, and completely dry it at 120°C for 2 hr.
10. Deep clean the substrate for 3 min using an oxygen plasma system.
11. Prepare a 2% (v/v) PFDS silane solution in 2,2,4-trimethylpentane and apply 200 μl onto the patterned area of the glass substrate. Apply a thin glass coverslip to cover the silane solution and incubate the reaction for 30 min.

    Note that trapped air bubbles between the substrate and coverslip may generate inconsistent surface properties. Bubbles can be removed by gently sliding the two slides to allow the bubble to escape out.
12. Remove the coverslip and rinse the substrate with 2,2,4-trimethylpentane to remove the PFDS residue, following by quenching of the silane by putting the substrate in 100% ethanol for 10 min. Rinse the substrate with water and dry with nitrogen.
13. Check the hydrophobicity of the exposed glass area.

    This area should be highly hydrophobic.
14. Glue the substrate with a glass spacer using a two-component epoxy. Cure the epoxy at 70°C overnight.
15. Etch the remaining chromium with chrome etchant until the patterns are fully transparent.

    After chromium removal, the newly exposed regions are hydrophilic due to the protection of the chromium layer.
16. Deep clean the chip by sonicating it in 1% Liquinox solution for 30 min, followed by multiple rinsing steps with purified water.
17. Dry the chip with nitrogen, and the chip is ready to use.

LIQUID CHROMATOGRAPHY AND MASS SPECTROMETRY

BASIC PROTOCOL 5

Nanoflow liquid chromatography combined with mass spectrometry (nanoLC-MS) is the method of choice for current proteomics data acquisition. LC provides the highest peak capacity and separation resolution for tryptic peptides. It is fully automated, which enables hundreds of samples to be analyzed in a reasonable time. Although the sensitivity

of LC-MS is inversely proportional to the flow rates of nanoLC (Yi, Piehowski, Shi, Smith, & Qian, 2017; Zhu, Zhao et al., 2018), the ultra-low flow-rate LC systems using narrow-i.d. columns (e.g., 20 μm i.d.) suffer from low robustness. To balance sensitivity and robustness, we employed 50-μm-i.d. columns in our study. We also designed and assembled an autosampler to directly integrate the nanoPOTS chip with LC-MS (Williams et al., 2020).

In terms of MS, high-resolution Orbitrap instruments such as Q-Extractive (HF) and Tribrid Lumos MS are commonly used in proteomic studies. To obtain optimal proteome coverage for a small number of plant cells, we choose Tribrid Lumos MS because it provides better sensitivity and scan speed. Here we describe an optimized LC and MS protocol for high-throughput and high-sensitivity analysis of LCM-isolated plant cells prepared by nanoPOTS.

Materials

Peptide samples (see protocols above)
QC peptide sample: e.g., HeLa digest (Thermo Fisher, cat. no. 88329)
Mobile Phase A (Buffer A); 0.1% formic acid in the water, Optima LC/MS Grade (Fisher Scientific)
Mobile Phase B (Buffer B): 0.1% formic acid in acetonitrile, Optima LC/MS Grade (Fisher Scientific)

LC columns (50 μm-i.d., 50 cm long), in-house packed with C18, 300 Å, 3-μm porous particles (Phenomenex, Torrance, CA) using a self-pack picofrit bare column (cat. no. PF360-50-10-N-5) purchased from New Objective (Littleton, MA). The pre-packed column can also be purchased from CoAnn Technologies, LLC, Richland, WA.
Capillary solid-phase extraction (SPE) column (100 μm-i.d., 4 cm long), in-house packed with C18, 300 Å, 5-μm porous particles (Phenomenex, Torrance, CA). The SPE column can also be purchased from CoAnn Technologies, LLC, Richland, WA.
Capillary column heater (AgileSleeve+, 40 cm × 1/32”, Analytical Sales and Services, Flanders, NJ)
Lumos Orbitrap MS (Thermo Fisher Scientific)
MSConvert (Chambers et al., 2012)
MSGFPlus/MASIC Data Processing Toolbox (downloaded from *https://github.com/PNNL-Comp-Mass-Spec/MSGFPlus_MASIC_Toolbox*)
MAGE (downloaded from *https://github.com/PNNL-Comp-Mass-Spec/Mage*)
SQL Server (Microsoft, Redmond, WA)
InfernoRDN (downloaded from *https://github.com/PNNL-Comp-Mass-Spec/InfernoRDN*)

LC-MS analysis procedures

1. Assemble LC column in a capillary column heater and set the column temperature to 50°C.

2. Equilibrate LC column and SPE column before sample injection.

   If a new LC/SPE column is used, a blank injection and gradient separation should be performed to activate the C18 particles.

3. Benchmark the performance of the LC-MS platform using a quality control (QC) peptide.

   The present LC-MS setup should be able to identify ∼15000 unique peptides and ∼2500 proteins by injecting 10-ng peptide mixtures. If significantly lower peptide and protein identifications (e.g., <12000 peptides and 2000 proteins) are observed, the user should

Table 1 The LC Gradient Profiles During Sample Loading and Sample Separation Steps

Pump	Steps	Time (min)	Flow rate (nl/min)	%Buffer B
Loading pump	1	0	3000	0
Loading pump	2	10	3000	0
Loading pump	3	12	0	0
Gradient Pump	4	12	150	2
Gradient Pump	5	14	150	8
Gradient Pump	6	112	150	22
Gradient Pump	7	132	150	35
Gradient Pump	8	137	150	80
Gradient Pump	9	147	150	80
Gradient Pump	10	148	150	2
Gradient Pump	11	162	150	2

replace LC and SPE columns, or perform a deep clean of the MS following the directions from the vendor.

4. Set up LC gradient method based on Table 1.

   Two pumps are used in the LC setup: one microflow pump for sample loading and one nanoflow pump for gradient separation.

5. The separated peptides are ionized by nano electrospray and collected by a Lumos Orbitrap MS operated under data-dependent acquisition mode. The MS acquisition method is listed in Table 2.

MS/MS data search procedure

6. Convert the MS/MS spectra from all LC-MS/MS datasets to ASCII text (`.dta` format) using MSConvert, which attempts to assign the appropriate charge and parent mass values to an MS/MS spectrum.

7. Interrogate the data files with MSGF+ (Kim & Pevzner, 2014) using a $\pm$ 20 ppm parent mass tolerance, partial tryptic enzyme settings, and a variable post-translational modification of oxidized methionine (+15.9949 Da) and static alkylation of cysteine (+57.0215 Da).

8. Use a target-decoy approach (Elias & Gygi, 2010) against available genome sequences of *P. tremula* $\times$ *P. alba* 717-1B4 (Kersten et al., 2016; Mader et al., 2016) and *Populus trichocarpa* (Tuskan et al., 2006), combined with typically observed contaminant proteins (keratins, trypsin, etc.).

9. Collate all MS/MS search results for a single LC-MS/MS dataset into a tab-separated ASCII text file listing the best scoring identification for each spectrum.

Data analysis procedure

10. Collate all MS/MS search results for each LC-MS/MS dataset into a tab-delimited text file using the in-house program MAGE Extractor. Import those results into a SQL Server (Microsoft, Redmond, WA) database and filter to 1% FDR by adjusting the *Q*-value provided by MSGF+.

11. Use the in-house program MASIC (Monroe, Shaw, Daly, Adkins, & Smith, 2008) on each LC-MS/MS dataset to provide a selected ion chromatogram (SIC, termed StatMomentsArea) for subsequent peptide quantitation steps.

Table 2 MS Acquisition Parameter for Highly Sensitive Proteomic Profiling of Small Numbers of Cells

Method Settings	
Application mode	Peptide
Method duration (min)	140
Ion Source	
Ion source type	NSI
Spray voltage	Static
Positive ion (V)	2200
MS global settings	
Infusion mode	Liquid chromatography
Expected LC peak width (s)	30
Default charge state	2
Advanced peak detection	True
Data-dependent mode: cycle time (s)	3
Master Scan/MS1 scan	
Detector type	Orbitrap
Orbitrap resolution	120000
Mass range	Normal
Use quadrupole isolation	True
Scan range (*m*/*z*)	375-1600
RF Lens	30
Normalized AGC target (%)	250
Maximum Injection Time (ms)	118
Microscan	1
Data type	Profile
Polarity	Positive
Filters	
MIPS: Monoisotopic Peak Determination	Peptide
Intensity threshold	2.0e4
ddMS2 scan	
Isolation mode	Quadrupole
Isolation window (*m*/*z*)	1.4
Isolation offset	Off
Activation type	HCD
Collision energy mode	Fixed
HCD collision energy (%)	30
Detector type	Ion trap
Ion trap scan rate	Rapid
Mass range	Normal
Scan range mode	Auto
Normalized AGC target (%)	200
Maximum Injection Time (ms)	150
Microscan	1
Data type	Centroid

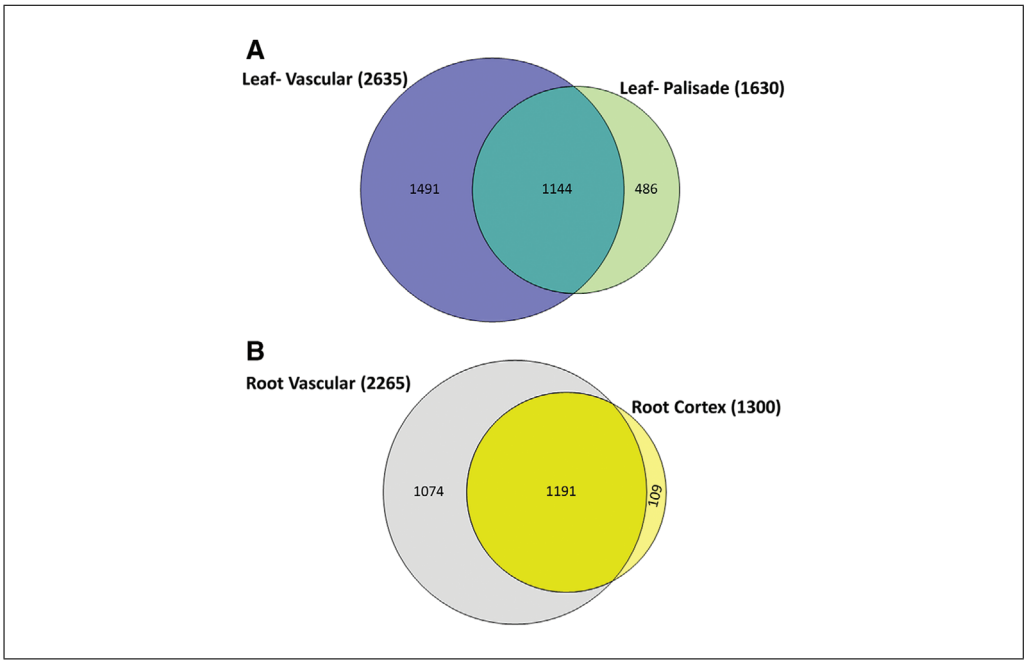

Figure 3 Venn diagram showing total number of proteins identified from poplar (**A**) leaf cells (palisade and vascular) and (**B**) root cells (cortex and vascular). These proteins are classified into cell-type-unique and -shared proteins.

12. Collate the results from all datasets' MASIC output using the in-house program MAGE File Processor, resulting in a tab-delimited file. Import these results into SQL Server (Microsoft, Redmond, WA) and connect to the filtered MSGF+ results via Dataset ID (internal to PNNL's data management system) and relevant MS/MS scan number and charge state.

13. Associate the peptide sequences with the first protein entry in the search FASTA (with post-translational modifications counted as separate sequences) and sum the StatMomentsArea values per grouped dataset.

14. Pivot these data to provide a crosstab of peptides, with protein information carried through. Import the crosstab into InfernoRDN (an implementation of the R statistical package; Polpitiya et al., 2008) and transform into Log_2 values.

15. Perform normalization of the peptide abundances using the mean central tendency (MCT) normalization approach (boxplot alignment) to remove experimentally induced bias.

    The data for this experiment had biases that were too large for MCT adjustment, so Median Absolute Deviation (MAD) normalization was applied before the MCT normalization.

16. Import the normalized peptide abundance values back into SQL Server, anti-log them, group the proteins, and sum the peptide abundances for each LC-MS/MS dataset. Finally, Log_2 transform the protein abundance values and pivot across all datasets to provide a protein crosstab.

17. Average the biological replicates, with minimum observation requirements adjusted to the number of replicates available. Count the proteins that pass the average Log_2 abundance values and compare between cell types to identify unique and shared protein numbers (Fig. 3).

18. Calculate a limit of reliable detection (LOD) for the averaged protein values within each compared sample such that a protein's abundance value that falls below two

standard deviations from the mean abundance within the compared sample is considered not to pass the LOD test.

19. As part of the example described in this article, the data are generated from poplar plants grown under normal conditions. In the case of comparing the datasets generated from two different experimental conditions, such as control vs. stress treatment, follow additional data analysis procedures listed below.

20. Subtract the averaged abundance values for relevant protein comparisons to provide log-ratios, and use the *Z*-score approach to assess the log-ratios using the formula [(log ratio of relevant protein) – (mean log ratio of total proteins)]/(standard deviation of log ratio of total proteins)].

21. Finally, assess the protein's behavior within a given comparison (e.g., control vs. stress treatment) using additional significance criteria such as (a) if a protein's *Z*-score is greater than 2 or less than −2; (b) if abundance value in both comparisons pass the LOD test; (c) if at least two unique peptides are observed for a relevant protein; or (d) if it is present in only one or the other compared condition.

For more rigorous statistical analysis, use ANOVA to derive a p-value for difference in foldchange between relevant comparisons.

COMMENTARY

Background Information

With the completion of genome sequencing in model species and strategic food and bioenergy crops, attention has been focused on linking genomic data and transcriptomic profiles to the spatiotemporal functional network of proteins (Hu, Rampitsch, & Bykova, 2015). Proteomics provides a critical source of information on biological systems through decoding the concentrations, functions, and catalytic activities of proteins as the major group of biological regulators (Baginsky, 2009). Several studies have performed proteomics analysis to identify proteins and characterize the post-translational modifications and protein-protein interactions at whole plant tissue levels (flower, leaf, stem, root) during plant developmental processes and responses to abiotic (Hashiguchi and Komatsu, 2016; Komatsu & Hossain, 2013) and biotic (Liu et al., 2019) stresses. However, plant responses to environmental perturbations are dynamic and involve complex crosstalk between different regulatory pathways (Shaar-Moshe, Blumwald, & Peleg, 2017), including protein expression at cellular levels for physiological and morphological adaptation at the whole-plant level (Krasensky & Jonak, 2012). Therefore, a cell-type-specific proteomics approach is needed to effectively reveal the underlying molecular mechanisms regulating developmental processes and plasticity.

Plant cell-type-specific proteomic studies initially started with cell suspension cultures, in which de-differentiated cells grown in liquid cultures were used to profile proteomic composition. This approach identified 573, 1367, and 3796 proteins in Arabidopsis (Böhmer & Schroeder, 2011), *Medicago truncatula* (Lei et al., 2005), and *Halogeton glomeratus* (Wang et al., 2016) cell cultures, respectively, depending on the analytical platforms used. Proteomic studies later focused on individual cell types such as pollen grains (Dai et al., 2006; Sheoran, Ross, Olson, & Sawhney, 2007; Zou et al., 2009), trichomes (Schilmiller et al., 2010; Van Cutsem et al., 2011), guard cells (Shao, Chu, Jaleel, & Zhao, 2008; Zhu, Dai, McClung, Yan, & Chen, 2009), and root hairs (Shao et al., 2008; Zhu et al., 2009). These efforts led to identifying a few hundreds to thousands of proteins per respective cell type (Dai & Chen, 2012).

Most available plant cell-type-specific harvesting methods are based on cell appearance/location, molecular markers, or other distinguishing properties (Nelson, Tausta, Gandotra, & Liu, 2006). For example, fluorescence-activated cell sorting (FACS) of protoplasts from dissociated tissues (Birnbaum et al., 2003) relies on the availability of specific markers (e.g., cell-type-specific promoters driving GFP). Compared with FACS, LCM is capable of harvesting most cell targets from histological sections of plant tissues (Emmert-Buck et al., 1996; Nelson et al., 2006; Day, Grossniklaus, & Macknight, 2005). LCM has been widely used to isolate cell types from complex plant tissues for multiple multiomics analysis, including

transcriptomics (Matas et al., 2011; Sui et al., 2018) and proteomics (Dembinsky et al., 2007; Zhu et al., 2016). So far, in cell-type-specific proteomics, LCM has been used to isolate cells from tomato root tissue (pericycle, root cortex, root epidermis; Dembinsky et al., 2007; Zhu et al., 2016), Arabidopsis stem (vascular cell type), and maize kernel (black layer, endosperm, and inner epidermis of pedicel). In Arabidopsis, from 400 vascular bundles isolated from stem comprising about 20000 cells, a total of 49 proteins were detected using mass spectrometry (Schad, Lipton, Giavalisco, Smith, & Kehr, 2005). In tomato (Zhu et al., 2016), the effect of aluminum treatment on epidermal and cortex cell types was studied in 5000-7000 cells per cell type, which resulted in the identification of 1313 and 744 proteins in each cell type, respectively. From the same cell types, with an improvement in the protein extraction method, a total of 3879 proteins were detected from pooled 80,000-100,000 cells of epidermis and cortex cell types (Yang et al., 2020). In another study with maize roots (Dembinsky et al., 2007), 1000 rings of root pericycle were LCM-dissected, containing approximately 200,000 cells, which yielded 30 μg of proteins that were run on 2-D gel. 56 protein spots were picked and analyzed using mass spectrometry. In maize seed kernel, several cell types such as black layer, endosperm cells, and inner epidermal cells were dissected with LCM, which yielded 41, 104, and 120 cell-type-specific proteins (Chen et al., 2020). In all of the above LCM-based proteomics studies, the protein identifications relied on many factors, including the number of dissected cells, protein loss during sample preparation, and the sensitivity of the mass spectrometry instrumentation.

Recent developments in small-volume sample preparation techniques such as NanoPOTS have helped increase the protein coverage up to 500 proteins from a minimum of 15 parenchyma cells isolated from tomato fruit tissue (Liang et al., 2018). The nanoPOTS platform is also applied to analyze single mammalian cells and reliably identify 600–1000 proteins from single culture HeLa cells (Cong et al., 2021; Zhu, Clair et al., 2018). We also integrated nanoPOTS with isobaric labeling approaches to improve the throughput of single-cell proteomics analyses. We demonstrated that ∼1500 proteins could be quantified across 152 single cells at a throughput of 77 cells per day (Tsai et al., 2020; Williams et al., 2020).

Critical Parameters and Troubleshooting

There are some critical parameters associated with tissue preparation for embedding in CMC reagent and handling the embedded blocks to obtain good cryosections during the cryosectioning process. For nanoPOTS-based protein digestion, enzyme amounts in nanowells should be adjusted according to different cell types. The MS parameters can be also improved if higher sensitivity is required.

Basic Protocol 1

Several embedding reagents are available, including paraffin wax, CMC (carboxymethylcellulose), and OCT (optimal cutting temperature compound). Paraffin is the most widely used embedding reagent in histological studies, as it provides sufficient resolution in tissue morphology; however, it suffers from longer embedding time and reduced turnover of biomolecules (Evers, He, Kim, Mason, & O'Leary, 2011). Paraffin is commonly used for formalin-fixed embedded tissues for long-term preservation at room temperature. The formalin fixation can cross-link the proteins and result in additional challenges during proteomic analysis. On the other hand, OCT is a well-established embedding medium for fresh-frozen tissues, which has been widely used in genomic studies, including cell-type specific RNA sequencing (Martin et al., 2016). However, OCT is not the optimal option for proteomics studies due to ion suppression and ionization competition in mass spectrometry analysis (rigorous washing steps are required before cell isolation and proteomic sample preparation; Shah et al., 2015). Although CMC does not preserve tissue morphology at a similar level to paraffin, it results in acceptable tissue morphology with high yield and integrity of biomolecules (Ishimaru et al., 2007). Moreover, hydroxypropyl methylcellulose (HPMC) is a substituted cellulosic polymer that can be used as an alternate embedding material to CMC (Dannhorn et al., 2020). During the embedding process, the tissue should be placed in the center and thoroughly covered with CMC. Sometimes the tissue floats onto the surface due to the less viscous nature of 2.5% CMC, which could create problems during cryosectioning. Also, if air bubbles are present near the tissue surface during the embedding step, the tissue can be gently moved using a spatula. The presence of air bubbles can interfere with obtaining good cryosections.

Basic Protocol 2

During cryosectioning, maintaining the mounting stage and blade temperature is critical to obtain good cryosections. For sectioning using CMC blocks, we adjusted the mounting stage temperature to −14°C and the blade temperature to −12°C. If the temperature gets colder, the CMC sections could crumble, which interferes with obtaining good cryosections. Moreover, adjusting the glass handle pressure is very important to get a good cryosection. When the sections break during the cryosectioning process, a little pressure can be applied to the glass handle, which helps in obtaining an intact cryosection.

Basic Protocol 3

The nanoliter DMSO droplets may evaporate slowly during the LCM process, which could negatively impact the sample collection efficiency. To facilitate the sample collection process, the selected areas on tissue sections should be cut first. Next, the nanowell chip is mounted on the LCM system to initiate the catapult process.

Depending on the tissue types and the nature of the plant species, LCM laser energy and the cycle number should be optimized to enable a more straightforward catapulting process.

Basic Protocol 4

Plant cells are heterogeneous, and the protein amounts in different cell types are highly variable depending on developmental stages and cell locations. We have found that both enzyme concentrations and protein-to-enzyme ratios are essential to ensure good digestion efficiency. In the current protocol, we used 0.5 ng Lys-C and 1 ng trypsin for digestion. This condition is appliable to samples containing 10 to 1000 plant cells, corresponding to 1 to 50 ng total proteins. If higher numbers of cells are isolated and cells containing high amounts of proteins are used, the enzyme amounts should be proportionally increased to maintain protein-to-enzyme ratios below 10.

For applications involving plant-pathogen interactions, the cell lysis protocol should be modified to allow efficient protein extraction for both plant and microbial cells. We found that increasing the cell lysis temperature to 95°C is sufficient to lyse most microbes.

Basic Protocol 5

During data-dependent acquisition (DDA), the proteome coverage is mainly determined by the ion injection times (IT) for the MS/MS scan. Generally, high ITs correspond to increased sensitivity by allowing long ion accumulation. However, it also leads to reduced MS scan speed. In this protocol, a moderate IT of 150 ms is suggested. If necessary, the IT can be increased to 500 ms for enhanced sensitivity for a low number of cells, such as single cells. Similarly, we can reduce the IT to increase MS scan speed for higher proteome coverage for large numbers of cells.

Understanding Results

Several studies showed that different plant cell types have unique molecular signatures that determine their differentiated functions (Ryu et al., 2019; Tang & Tang, 2019; Yuan et al., 2018). Advancement in proteomics analysis of small numbers of cells enabled the identification of cell type-specific proteins with important roles in plant biological processes (Dembinsky et al., 2007; Petricka et al., 2012; Zhu et al., 2016). Here, we present an optimized step-by-step protocol to perform a high-throughput quantification of protein abundances in four major cell types of poplar leaf (palisade and vascular) and root (cortex and vascular) tissues. Understanding the proteomic composition of specific cell types provides information that is missing in whole tissue−based analyses, including cell population−specific protein profiles that are unique for the distinct cellular layers of leaves and roots.

In leaf tissue, we identified 1630 proteins from palisade cells (out of 500-1000 isolated cells) and 2635 proteins from vascular cells (out of 1000-2000 isolated cells; Fig. 3). In root tissue, however, we identified 1300 proteins from cortex cells (out of 500-1000 cells) and 2265 proteins from vascular cells (out of 1000-2000 cells). To generate the list, we required these proteins to have more than one matched peptide, to be detected in more than 50% of replicates, and to have successfully passed the LOD abundance filter analysis [abundance values greater than 2 standard deviations below the mean of the averaged abundances (LOD test value =1) (Liang et al., 2018)]. Among these, 486 (in leaf palisade), 1491 (in leaf vascular), 109 (in root cortex), and 1074 (in root vascular) proteins were identified as unique cell-type-specific proteins (Fig. 3 and supplementary table 1). Our biological pathway analysis using the Fisher exact test ($p < .05$; PoplarCYC v12 *https://plantcyc.org/content/poplarcyc-12.0* and Plant Metabolic Network (PMN; Karp

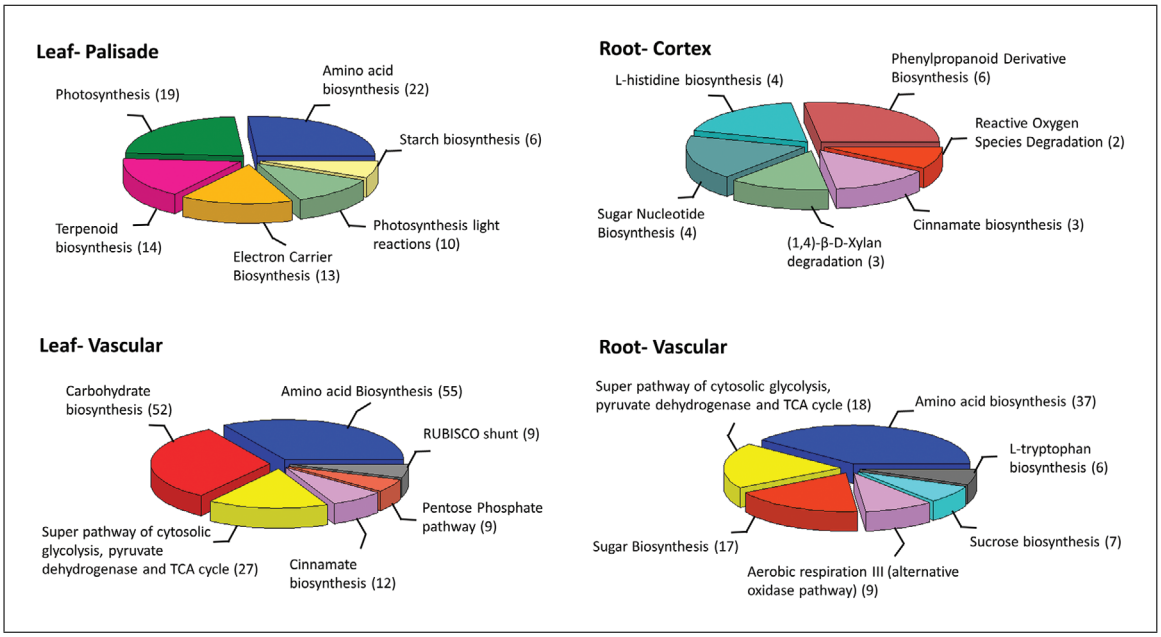

Figure 4 Unique cell-type-specific proteins from leaf (palisade and vascular) and root (cortex and vascular) tissues were used to perform pathway enrichment analysis with PoplarCYC v11 and Plant Metabolic Network (PMN; which uses Fisher exact statistics with $p < .05$). The most significant enriched pathways are shown here. The number of enriched proteins are shown in parenthesis.

Table 3 Time Considerations for Basic Protocols

Step no.	Protocols	Time required
1.	Tissue harvest and fixation	30 min–1 hr
2.	Cryoprotection and embedding in CMC reagent	5–6 hr
3.	Cryosectioning of embedded CMC blocks	1 hr per tissue block
4.	Laser capture microdissection	3-4 hr for leaf and 2-3 hr for root (per tissue section)
5.	Microchip fabrication	2 days total time for up to 10 chips
6.	NanoPOTS-based sample preparation	2 days total time for up to 10 chips and 270 samples
7.	Liquid chromatography and mass spectrometry	2.5 hr per sample

et al., 2016) identified several significantly enriched cell-type specific pathways in both leaf and root tissues (Fig. 4).

Among unique palisade cell type specific proteins, 92 proteins were significantly enriched in several biological pathways, including amino acid biosynthesis (24%), photosynthesis (21%), terpenoid biosynthesis (15%), electron carrier biosynthesis (14%), photosynthesis light reaction (11%), and starch biosynthesis (6%). In leaf vascular cells, 241 proteins were significantly enriched in several pathways categorized into amino acid biosynthesis (22%), carbohydrate biosynthesis (21%), super pathway of cytosolic glycolysis, pyruvate dehydrogenase and TCA cycle (11%), cinnamate biosynthesis (5%), pentose phosphate pathway (4%), and rubisco shunt (4%). Overall, the protein composition in leaf tissue indicated photosynthesis-related proteins as major components of palisade cells, while proteins involved in carbohydrate and sugar biosynthesis were more abundant in vascular cells.

Root cortex cells showed 19 enriched proteins out of the 109 identified unique proteins classified into phenylpropanoid derivative biosynthesis (32%), L-histidine biosynthesis (21%), sugar nucleotide biosynthesis (21%), (1,4)-β-D-xylan degradation (15%), cinnamate biosynthesis (15%), and reactive oxygen species (ROS) degradation (11%). Among unique root vascular proteins, 127 proteins were significantly enriched in different biological pathways related to amino acid biosynthesis (29%), super pathway of cytosolic glycolysis, pyruvate dehydrogenase,

and TCA cycle (14%), sugar biosynthesis (13%), aerobic respiration III (alternative oxidase pathway; 7%), sucrose biosynthesis (6%), and L-tryptophan biosynthesis (5%). The enrichment of phenolic compounds and sugar biosynthetic proteins in root cortex cells indicates a possible storage-related function. However, vascular root cells, similar to leaf vascular cells, were mainly enriched in amino acid and sugar biosynthetic pathways, suggesting possible shared metabolic processes within vascular cells in leaf and root tissues.

Time Considerations

Table 3 shows time considerations for the different procedure in this article.

Acknowledgments

The authors thank Dr. Stephen DiFazio (West Virginia University) for providing the original Poplar clones used in this study and Tanya Winkler (EMSL, PNNL) for helping in clonal propagation of poplars. The authors also want to thank PNNL Graphic Designer Nathan Johnson and photographer Andrea Starr for preparing Figure 1. This work was supported by funding from the Biological and Environmental Research (BER) in the U.S. Department of Energy (DOE) Office of Science, Genomic Science Program, Biosystems Design to Enable Next-Generation Biofuels (SyPro project, Award Number: DE-SC0018347). This research was supported by an intramural program at EMSL (grid.436923.9), a DOE Office of Science User Facility sponsored by the Office of Biological and Environmental Research and operated under Contract No. DE-AC05-76RL01830, located at Pacific Northwest National Laboratory (PNNL).

Author Contributions

Vimal Balasubramanian: conceptualization, data curation, formal analysis, investigation, methodology, writing original draft, writing review and editing. **Samuel Purvine:** data curation, formal analysis, investigation, methodology, software, writing original draft, writing review and editing. **Yiran Liang:** investigation, methodology, writing original draft, writing review and editing. **Ryan Kelly:** writing review and editing. **Ljiljana Pasa-Tolic:** resources, supervision, writing review and editing. **William Chrisler:** investigation, methodology, writing review and editing. **Eduardo Blumwald:** funding acquisition, investigation, project administration, writing review and editing. **C. Neal Stewart:** funding acquisition, project administration, writing review and editing. **Ying Zhu:** conceptualization, data curation, formal analysis, funding acquisition, investigation, methodology, supervision, writing original draft, writing review and editing. **Amir H. Ahkami:** conceptualization, data curation, formal analysis, funding acquisition, investigation, methodology, project administration, supervision, writing original draft, writing review and editing.

Conflict of Interest

The authors declare no competing financial interest.

Data Availability Statement

Data sharing not applicable—no new data generated.

Literature Cited

Ahram, M., Flaig, M. J., Gillespie, J. W., Duray, P. H., Linehan, W. M., Ornstein, D. K. … Emmert-Buck, M. R. (2003). Evaluation of ethanol-fixed, paraffin-embedded tissues for proteomic applications. *Proteomics*, *3*, 413–421. doi: 10.1002/pmic.200390056.

Baginsky, S. (2009). Plant proteomics: Concepts, applications, and novel strategies for data interpretation. *Mass Spectrometry Reviews*, *28*, 93–120. doi: 10.1002/mas.20183.

Birnbaum, K., Shasha, D. E., Wang, J. Y., Jung, J. W., Lambert, G. M., Galbraith, D. W., & Benfey P. N. (2003). A gene expression map of the Arabidopsis root. *Science*, *302*, 1956–1960. doi: 10.1126/science.1090022.

Böhmer, M., & Schroeder, J. I. (2011). Quantitative transcriptomic analysis of abscisic acid-induced and reactive oxygen species-dependent expression changes and proteomic profiling in Arabidopsis suspension cells. *Plant Journal*, *67*, 105–118. doi: 10.1111/j.1365-313X.2011.04579.x.

Chambers, M. C., Maclean, B., Burke, R., Amodei, D., Ruderman, D. L., Neumann, S. … Mallick, P. (2012). A cross-platform toolkit for mass spectrometry and proteomics. *Nature Biotechnology*, *30*, 918–920. doi: 10.1038/nbt.2377.

Chen, Q., Huang, R., Xu, Z., Zhang, Y., Li, L., Fu, J. … Gu, R. (2020). Label-free comparative proteomic analysis combined with laser-capture microdissection suggests important roles of stress responses in the black layer of maize kernels. *International Journal of Molecular Sciences*, *21*(4), 1369. doi: 10.3390/ijms21041369.

Collado-Romero, M., Alós, E., & Prieto, P. (2014). Unravelling the proteomic profile of rice meiocytes during early meiosis. *Frontiers in Plant Science*, *5*, 356–356. doi: 10.3389/fpls.2014.00356.

Cong, Y., Motamedchaboki, K., Misal, S. A., Liang, Y., Guise, A. J., Truong, T. … Kelly, R. T. (2021). Ultrasensitive single-cell proteomics workflow identifies >1000 protein groups per

mammalian cell. *Chemical Science*, *12*, 1001–1006. doi: 10.1039/D0SC03636F.

Dai, S., & Chen, S. (2012). Single-cell-type proteomics: Toward a holistic understanding of plant function. *Molecular and Cellular Proteomics*, *11*, 1622–1630. doi: 10.1074/mcp.R112.021550.

Dai, S., Li, L., Chen, T., Chong, K., Xue, Y., & Wang, T. (2006). Proteomic analyses of *Oryza sativa* mature pollen reveal novel proteins associated with pollen germination and tube growth. *Proteomics*, *6*, 2504–2529. doi: 10.1002/pmic.200401351.

Dannhorn, A., Kazanc, E., Ling, S., Nikula, C., Karali, E., Serra, M. P. … Takats, Z. (2020). Universal sample preparation unlocking multimodal molecular tissue imaging. *Analytical Chemistry*, *92*, 11080–11088. doi: 10.1021/acs.analchem.0c00826.

Day, R. C., Grossniklaus, U., & Macknight, R. C. (2005). Be more specific! Laser-assisted microdissection of plant cells. *Trends in Plant Science*, *10*, 397–406. doi: 10.1016/j.tplants.2005.06.006.

Dembinsky, D., Woll, K., Saleem, M., Liu, Y., Fu, Y., Borsuk, L. A. … Hochholdinger, F. (2007). Transcriptomic and proteomic analyses of pericycle cells of the maize primary root. *Plant Physiology*, *145*, 575–588. doi: 10.1104/pp.107.106203.

Dou, M., Tsai, C.-F., Piehowski, P. D., Wang, Y., Fillmore, T. L., Zhao, R. … Zhu, Y. (2019). Automated nanoflow two-dimensional reversed-phase liquid chromatography system enables in-depth proteome and phosphoproteome profiling of nanoscale samples. *Analytical Chemistry*, *91*, 9707–9715. doi: 10.1021/acs.analchem.9b01248.

Elias, J. E., & Gygi, S. P. (2010). Target-decoy search strategy for mass spectrometry-based proteomics. *Methods in Molecular Biology*, *604*, 55–71. doi: 10.1007/978-1-60761-444-9_5.

Emmert-Buck, M. R., Bonner, R. F., Smith, P. D., Chuaqui, R. F., Zhuang, Z., Goldstein, S. R. … Liotta L. A. (1996). Laser capture microdissection. *Science*, *274*, 998–1001. doi: 10.1126/science.274.5289.998.

Evers, D. L., He, J., Kim, Y. H., Mason, J. T., & O'Leary, T. J. (2011). Paraffin embedding contributes to RNA aggregation, reduced RNA yield, and low RNA quality. *The Journal of Molecular Diagnostics*, *13*, 687–694. doi: 10.1016/j.jmoldx.2011.06.007.

Hashiguchi, A., & Komatsu, S. (2016). Impact of post-translational modifications of crop proteins under abiotic stress. *Proteomes*, *4*, 42. doi: 10.3390/proteomes4040042.

Hölscher, D., & Schneider, B. (2008). Application of laser-assisted microdissection for tissue and cell-specific analysis of RNA, proteins, and metabolites. In U. Lüttge, W. Beyschlag, & J. Murata (Eds.), *Progress in Botany* (pp. 141–167). Berlin, Heidelberg: Springer Berlin Heidelberg.

Hu, J., Rampitsch, C., & Bykova, N. V. (2015). Advances in plant proteomics toward improvement of crop productivity and stress resistance. *Frontiers in Plant Science*, *6*, 209–209. doi: 10.3389/fpls.2015.00209.

Ishimaru, T., Nakazono, M., Masumura, T., Abiko, M., San-oh, Y., Nishizawa, N. K., & Kondo, M. (2007). A method for obtaining high integrity RNA from developing aleurone cells and starchy endosperm in rice (*Oryza sativa* L.) by laser microdissection. *Plant Science*, *173*, 321–326. doi: 10.1016/j.plantsci.2007.06.004.

Karp, P. D., Latendresse, M., Paley, S. M., Krummenacker, M., Ong, Q. D., Billington, R. … Caspi R. (2016). Pathway Tools version 19.0 update: Software for pathway/genome informatics and systems biology. *Briefings in Bioinformatics*, *17*, 877–890. doi: 10.1093/bib/bbv079.

Kersten, B., Faivre Rampant, P., Mader, M., Le Paslier, M. C., Bounon, R., Berard, A. … Fladung, M. (2016). Genome sequences of *Populus tremula* chloroplast and mitochondrion: Implications for holistic poplar breeding. *PloS One*, *11*, e0147209. doi: 10.1371/journal.pone.0147209.

Kim, S., & Pevzner, P. A. (2014). MS-GF+ makes progress towards a universal database search tool for proteomics. *Nature Communication*, *5*, 5277. doi: 10.1038/ncomms6277.

Komatsu, S., & Hossain, Z. (2013). Organ-specific proteome analysis for identification of abiotic stress response mechanism in crop. *Frontiers in Plant Science*, *4*, 71. doi: 10.3389/fpls.2013.00071.

Krasensky, J., & Jonak, C. (2012). Drought, salt, and temperature stress-induced metabolic rearrangements and regulatory networks. *Journal of Experimental Botany*, *63*, 1593–1608. doi: 10.1093/jxb/err460.

Lee, U. N., Su, X., Guckenberger, D. J., Dostie, A. M., Zhang, T., Berthier, E., & Theberge, A. B. (2018). Fundamentals of rapid injection molding for microfluidic cell-based assays. *Lab on a Chip*, *18*, 496–504. doi: 10.1039/C7LC01052D.

Lei, Z., Elmer, A. M., Watson, B. S., Dixon, R. A., Mendes, P. J., & Sumner, L. W. (2005). A two-dimensional electrophoresis proteomic reference map and systematic identification of 1367 proteins from a cell suspension culture of the model legume *Medicago truncatula*. *Molecular and Cellular Proteomics*, *4*, 1812–1825. doi: 10.1074/mcp.D500005-MCP200.

Liang, Y., Zhu, Y., Dou, M., Xu, K., Chu, R. K., Chrisler, W. B. … Kelly, R. T. (2018). Spatially resolved proteome profiling of <200 cells from tomato fruit pericarp by integrating laser-capture microdissection with nanodroplet sample preparation. *Analytical Chemistry*, *90*, 11106–11114. doi: 10.1021/acs.analchem.8b03005.

Libault, M., Pingault, L., Zogli, P., & Schiefelbein, J. (2017). Plant systems biology at the single-cell level. *Trends in Plant Science*, *22*, 949–960. doi: 10.1016/j.tplants.2017.08.006.

Liu, W. W., Zhu, Y., Feng, Y. M., Fang, J., & Fang, Q. (2017). Droplet-based multivolume digital polymerase chain reaction by a surface-assisted multifactor fluid segmentation approach. *Analytical Chemistry*, *89*, 822–829. doi: 10.1021/acs.analchem.6b03687.

Liu, Y., Lu, S., Liu, K., Wang, S., Huang, L., & Guo, L. (2019). Proteomics: A powerful tool to study plant responses to biotic stress. *Plant Methods*, *15*, 135. doi: 10.1186/s13007-019-0515-8.

Mader, M., Paslier, M.-C. Le, Bounon, R., Bérard, A., Rampant, P. F., Fladung, M. … Kersten, B. (2016). Whole-genome draft assembly of *Populus tremula* × *P. alba* clone INRA 717-1B4. *Silvae Genetica*, *65*, 74–79. doi: 10.1515/sg-2016-0019.

Marion, J., Bars, R. Le, Satiat-Jeunemaitre, B., & Boulogne, C. (2017). Optimizing CLEM protocols for plants cells: GMA embedding and cryosections as alternatives for preservation of GFP fluorescence in Arabidopsis roots. *Journal of Structural Biology*, *198*, 196–202. doi: 10.1016/j.jsb.2017.03.008.

Martin, L., Nicolas, P., Matas Arroyo, A., Shinozaki, Y., Catala, C., & Rose, J. (2016). Laser microdissection of tomato fruit cell and tissue types for transcriptome profiling. *Nature Protocols*, *11*, 2376–2388. doi: 10.1038/nprot.2016.146.

Matas, A. J., Yeats, T. H., Buda, G. J., Zheng, Y., Chatterjee, S., Tohge, T. … Rose, J. K. C. (2011). Tissue- and cell-type specific transcriptome profiling of expanding tomato fruit provides insights into metabolic and regulatory specialization and cuticle formation. *The Plant Cell*, *23*, 3893. doi: 10.1105/tpc.111.091173.

Milcheva, R., Janega, P., Celec, P., Russev, R., & Babál, P. (2013). Alcohol based fixatives provide excellent tissue morphology, protein immunoreactivity and RNA integrity in paraffin embedded tissue specimens. *Acta Histochemica*, *115*, 279–289. doi: 10.1016/j.acthis.2012.08.002.

Monroe, M. E., Shaw, J. L., Daly, D. S., Adkins, J. N., & Smith, R. D. (2008). MASIC: A software program for fast quantitation and flexible visualization of chromatographic profiles from detected LC–MS(/MS) features. *Computational Biology and Chemistry*, *32*, 215–217. doi: 10.1016/j.compbiolchem.2008.02.006.

Nelson, T., Tausta, S. L., Gandotra, N., & Liu, T. (2006). Laser microdissection of plant tissue: What you see is what you get. *Annual Review of Plant Biology*, *57*, 181–201. doi: 10.1146/annurev.arplant.56.032604.144138.

Nestler, J., Schütz, W., & Hochholdinger, F. (2011). Conserved and unique features of the maize (Zea mays L.) root hair proteome. *Journal of Proteome Research*, *10*, 2525–2537. doi: 10.1021/pr200003k.

Petricka, J. J., Schauer, M. A., Megraw, M., Breakfield, N. W., Thompson, J. W., Georgiev, S. … Benfey, P. N. (2012). The protein expression landscape of the Arabidopsis root. *Proceedings of the National Academy of Sciences*, *109*, 6811–6818. doi: 10.1073/pnas.1202546109.

Polpitiya, A. D., Qian, W.-J., Jaitly, N., Petyuk, V. A., Adkins, J. N., Camp, D. G., II … Smith, R. D. (2008). DAnTE: A statistical tool for quantitative analysis of -omics data. *Bioinformatics*, *24*, 1556–1558. doi: 10.1093/bioinformatics/btn217.

Rhee, S. Y., Birnbaum, K. D., & Ehrhardt, D. W. (2019). Towards building a plant cell atlas. *Trends in Plant Science*, *24*, 303–310. doi: 10.1016/j.tplants.2019.01.006.

Ryu, K. H., Huang, L., Kang, H. M., & Schiefelbein, J. (2019). Single-cell RNA sequencing resolves molecular relationships among individual plant cells. *Plant Physiology*, *179*, 1444–1456. doi: 10.1104/pp.18.01482.

Schad, M., Lipton, M. S., Giavalisco, P., Smith, R. D., & Kehr, J. (2005). Evaluation of two-dimensional electrophoresis and liquid chromatography – tandem mass spectrometry for tissue-specific protein profiling of laser-microdissected plant samples. *Electrophoresis*, *26*, 2729–2738. doi: 10.1002/elps.200410399.

Schilmiller, A. L., Miner, D. P., Larson, M., McDowell, E., Gang, D. R., Wilkerson, C., & Last, R. L. (2010). Studies of a biochemical factory: Tomato trichome deep expressed sequence tag sequencing and proteomics. *Plant Physiology*, *153*, 1212–1223. doi: 10.1104/pp.110.157214.

Shaar-Moshe, L., Blumwald, E., & Peleg, Z. (2017). Unique physiological and transcriptional shifts under combinations of salinity, drought, and heat. *Plant Physiology*, *174*, 421–434. doi: 10.1104/pp.17.00030.

Shah, P., Zhang, B., Choi, C., Yang, S., Zhou, J., Harlan, R. … Zhang, H. (2015). Tissue proteomics using chemical immobilization and mass spectrometry. *Analytical Biochemistry*, *469*, 27–33. doi: 10.1016/j.ab.2014.09.017.

Shao, H.-B., Chu, L.-Y., Jaleel, C. A., & Zhao, C.-X. (2008). Water-deficit stress-induced anatomical changes in higher plants. *Comptes Rendus Biologies*, *331*, 215–225. doi: 10.1016/j.crvi.2008.01.002.

Sheoran, I. S., Ross, A. R., Olson, D. J., & Sawhney, V. K. (2007). Proteomic analysis of tomato (*Lycopersicon esculentum*) pollen. *Journal of Experimental Botany*, *58*, 3525–3535. doi: 10.1093/jxb/erm199.

Slavov, N. (2020). Unpicking the proteome in single cells. *Science*, *367*, 512–513. doi: 10.1126/science.aaz6695.

Solomon, M. J., & Varshavsky, A. (1985). Formaldehyde-mediated DNA-protein crosslinking: A probe for in vivo chromatin structures. *Proceedings of the National Academy of Sciences of the United States of America*, *82*, 6470–6474. doi: 10.1073/pnas.82.19.6470.

Sui, X., Nie, J., Li, X., Scanlon, M. J., Zhang, C., Zheng, Y. … Zhang, Z. (2018). Transcriptomic and functional analysis of cucumber (*Cucumis*

sativus L.) fruit phloem during early development. *The Plant Journal*, *96*, 982–996. doi: 10.1111/tpj.14084.

Tang, W., & Tang, A. Y. (2019). Biological significance of RNA-seq and single-cell genomic research in woody plants. *Journal of Forestry Research*, *30*, 1555–1568. doi: 10.1007/s11676-019-00933-w.

Tsai, C. F., Zhao, R., Williams, S. M., Moore, R. J., Schultz, K., Chrisler, W. B. … Liu, T. (2020). An improved boosting to amplify signal with isobaric labeling (iBASIL) strategy for precise quantitative single-cell proteomics. *Molecular & Cellular Proteomics*, *19*, 828–838. doi: 10.1074/mcp.RA119.001857.

Tuskan, G. A., DiFazio, S., Jansson, S., Bohlmann, J., Grigoriev, I., Hellsten, U. … Rokhsar, D. (2006). The genome of black cottonwood, Populus trichocarpa (Torr. & Gray). *Science*, *313*, 1596–1604. doi: 10.1126/science.1128691.

Van Cutsem, E., Simonart, G., Degand, H., Faber, A. M., Morsomme, P., & Boutry, M. (2011). Gel-based and gel-free proteomic analysis of Nicotiana tabacum trichomes identifies proteins involved in secondary metabolism and in the (a)biotic stress response. *Proteomics*, *11*, 440–454. doi: 10.1002/pmic.201000356.

Wang, J., Yao, L., Li, B., Meng, Y., Ma, X., Lai, Y. … Wang, H. (2016). Comparative proteomic analysis of cultured suspension cells of the halophyte *Halogeton glomeratus* by iTRAQ provides insights into response mechanisms to salt stress. *Frontiers in Plant Science*, *7*, 110–110. doi: 10.3389/fpls.2016.00110.

Williams, S. M., Liyu, A. V., Tsai, C. F., Moore, R. J., Orton, D. J., Chrisler, W. B. … Zhu, Y. (2020). Automated coupling of nanodroplet sample preparation with liquid chromatography−mass spectrometry for high-throughput single-cell proteomics. *Analytical Chemistry*, *92*, 10588–10596. doi: 10.1021/acs.analchem.0c01551.

Yang, S., Li, H., Bhatti, S., Zhou, S., Yang, Y., Fish, T., & Thannhauser, T. W. (2020). The Al-induced proteomes of epidermal and outer cortical cells in root apex of cherry tomato 'LA 2710'. *Journal of Proteomics*, *211*, 103560. doi: 10.1016/j.jprot.2019.103560.

Yi, L., Piehowski, P. D., Shi, T., Smith, R. D., & Qian, W. J. (2017). Advances in microscale separations towards nanoproteomics applications. *Journal of Chromatography. A*, *1523*, 40–48. doi: 10.1016/j.chroma.2017.07.055.

Yuan, Y., Lee, H., Hu, H., Scheben, A., & Edwards, D. (2018). Single-cell genomic analysis in plants. *Genes (Basel)*, *9*, 50. doi: 10.3390/genes9010050.

Zhu, M., Dai, S., McClung, S., Yan, X., & Chen, S. (2009). Functional differentiation of *Brassica napus* guard cells and mesophyll cells revealed by comparative proteomics. *Molecular & Cellular Proteomics*, *8*, 752–766. doi: 10.1074/mcp.M800343-MCP200.

Zhu, Y., Clair, G., Chrisler, W. B., Shen, Y., Zhao, R., Shukla, A. K. … Kelly, R. T. (2018). Proteomic analysis of single mammalian cells enabled by microfluidic nanodroplet sample preparation and ultrasensitive NanoLC-MS. *Angewandte Chemie*, *57*, 12370–12374. doi: 10.1002/anie.201802843.

Zhu, Y., Dou, M., Piehowski, P. D., Liang, Y., Wang, F., Chu, R. K. … Kelly, R. T. (2018). Spatially resolved proteome mapping of laser capture microdissected tissue with automated sample transfer to nanodroplets. *Molecular & Cellular Proteomics*, *17*, 1864–1874. doi: 10.1074/mcp.TIR118.000686.

Zhu, Y., Li, H., Bhatti, S., Zhou, S., Yang, Y., Fish, T., & Thannhauser, T. W. (2016). Development of a laser capture microscope-based single-cell-type proteomics tool for studying proteomes of individual cell layers of plant roots. *Horticulture Research*, *3*, 16026. doi: 10.1038/hortres.2016.26.

Zhu, Y., Piehowski, P. D., Zhao, R., Chen, J., Shen, Y., Moore, R. J. … Kelly, R. T. (2018). Nanodroplet processing platform for deep and quantitative proteome profiling of 10-100 mammalian cells. *Nature Communications*, *9*, 882. doi: 10.1038/s41467-018-03367-w.

Zhu, Y., Zhao, R., Piehowski, P. D., Moore, R. J., Lim, S., Orphan, V. J. … Kelly, R. T. (2018). Subnanogram proteomics: Impact of LC column selection, MS instrumentation and data analysis strategy on proteome coverage for trace samples. *International Journal of Mass Spectrometry*, *427*, 4–10. doi: 10.1016/j.ijms.2017.08.016.

Zou, J., Song, L., Zhang, W., Wang, Y., Ruan, S., & Wu, W. H. (2009). Comparative proteomic analysis of Arabidopsis mature pollen and germinated pollen. *Journal of Integrative Plant Biology*, *51*, 438–455. doi: 10.1111/j.1744-7909.2009.00823.x.